Journal of Solid Mechanics Vol. 8, No. 3 (2016) pp. 511-529

Free Vibration Analysis of Microtubules as Orthotropic Elastic Shells Using Stress and Strain Gradient Elasticity Theory

F. Mokhtari [1], Y. Tadi Beni [2, *]

[1]*Faculty of Engineering, Shahrekord University, Shahrekord, Iran*
[2]*Nanotechnology Research Center, Shahrekord University, Shahrekord, Iran*

Received 30 May 2016; accepted 7 July 2016

ABSTRACT

In this paper, vibration of the protein microtubule, one of the most important intracellular elements serving as one of the common components among nanotechnology, biotechnology and mechanics, is investigated using stress and strain gradient elasticity theory and orthotropic elastic shells model. Microtubules in the cell are influenced by internal and external stimulation and play a part in conveying protein substances and taking medications to the intended targets. Therefore, in order to control the biological cell functions, it is important to know the vibrational behavior of microtubules. For this purpose, using the cylindrical shell model which fully corresponds to microtubule geometry, and by considering it as orthotropic which is closer to reality, based on gradient elasticity theory, frequency analysis of the protein microtubule is carried out by considering Love's thin shell theory and Navier solution. Also, the effect of size parameter and other variables on the results are investigated.

Keywords : Protein microtubule; Stress and strain gradient elasticity theory; Orthotropic elastic shells; Thin shell theory; Size effect.

1 INTRODUCTION

BIOMECHANICS is a new science which appeared in the recent years as mechanical engineering was becoming functional. Studying the biomechanics of living cells and biomolecules is significant for different reasons. Cell mechanics can considerably help to figure out how mechanical signals change and convert into intracellular biological and biochemical responses. If the relations between the mechanical medium of cells and tissues are identified, there will be much greater possibility to find a way to regulate the structure and function of these cells and tissues [1].

Protein microtubule or cellular micro tube is the most robust element of cytoskeleton, and, based on laboratory studies, is approximately 100 times as robust as other elements of the cytoskeleton [2]. Having polar properties, these nanotubes are polymers composed of microscopic sub-units. They are in the shape of hollow cylinders 25 and 15 nm in external and internal diameters, respectively. These fibers are known as self-assembled nanotubes able to increase or decrease in length in the 10 nm to 100 μm interval.

Structurally, microtubules are constructed by lateral connection of relatively long fibers known as protofilaments the number of which varies in different microtubules, causing geometric differences among microtubules [3,4].

*Corresponding author. Tel.: +98 381 4424438; Fax: +98 381 4424438.
E-mail address: *tadi@eng.sku.ac.ir* (Y.Tadi Beni).

Protofilaments are in turn constructed by successive connection of fundamental elements known as α and β tubulins. The α-tubulin represents the negative pole and the β-tubulin represents the positive pole in the microtubule [5].

Considering the vital role played by microtubules in many biological activities, studying their mechanical behavior is of considerable importance. One of the important properties of protein microtubules is their mechanical vibration, offering significant hallmarks for studying and investigating intracellular behaviors, of which one is protein microtubule frequency.

Considering its dimensions, the microtubule can be thought of as a biological nanostructure. Such structures must be investigated by considering the effect of small size [6]. This is done using higher order continuum theories [7-10]. In these theories, unlike the classical elasticity theory, stress in each node is not merely dependent on strain in the same node; rather, it is also a function of strain in other nodes as well [11, 12].

Numerous experiments and simulations have so far been conducted to study the mechanical behavior and properties of protein microtubules. With respect to the literature on protein microtubules, researchers to date have used various beam models to conduct frequency analysis of microtubules, often employing classical elasticity theory and ignoring effects of the small size [13-16]. In recent years, some researchers have employed Eringen's nonlocal theory [12] and other non-classical theories to study microtubule vibration by taking into account the effects of small size, either modeling the microtubule as a beam or assuming it as an isotropic shell. Wang & Ru [17] carried out frequency analysis of microtubule based on classical elasticity theory and using orthotropic cylindrical shell model, demonstrating that the frequencies resulting from the orthotropic model are considerably smaller than frequencies of the isotropic model. Using orthotropic cylindrical shell model and based on the classical elasticity theory, Zhang & Wang [18] studied microtubule vibration. Modeling microtubule as a nonlinear shear cylindrical shell and based on the Eringen's nonlocal theory, Shen [19] investigated the nonlocal vibration of protein microtubule and examined the effect of nonlocal parameter and cytoplasm medium on microtubule frequency. Civalek & Akgöz [20] used the nonlocal Euler-Bernoulli beam model to examine the effect of length, nonlocal parameter and support conditions on microtubule vibration. They demonstrated that increase in microtubule length and nonlocal parameter is accompanied by decrease in vibration frequency. Tounsi et al. [21] investigated microtubule vibration based on Eringen's nonlocal theory and using Timoshenko beam model. They examined the effect of the nonlocal parameter and shear modulus on microtubule vibration frequency. Liew and Xiang [22] employed atomistic-continuum model and strain gradient theory to carry out frequency analysis of microtubules. They demonstrated that increase in length is accompanied by decrease in microtubule frequency, and increase in size parameter is accompanied by increase in microtubule frequency. Karimi & Tadi Beni [23] analyzed the vibration of protein microtubules based on Euler-Bernoulli beam model and modified strain gradient theory, and investigated the effect of small size parameters and microtubule dimensions on the results.

Based on research done in the past on the nano-scale, it is well-established that mechanical behaviors of micro/nano structure are size dependent [24,25]. Experiments reveal an increase in material characteristics such as yield strength, hardness, bending rigidity, Young modulus, etc. with decreasing the size at the ultra-small scales [25-29]. All previous experimental studies imply that when the characteristic size (thickness, diameter, etc.) of a micro/nano element is in the order of its intrinsic material length scales (typically sub-micron), the material elastic constants highly depend on the element dimensions. Unfortunately, while much is known about the mechanical characteristics of isolated bulk materials, the properties of material at nano-scale cannot necessarily be predicted from those measured at larger scales. However, this problem can be resolved by the incorporation of an intrinsic material length scale parameter in the governing equations of continuum mechanics theory. Note that classical continuum mechanics is unable to simulate the size effect in micro/nano structures. One way to model the size dependency in micro/nano structures is using the atomistic methods such as molecular dynamics (MD). But, it is still not possible to conduct time-consuming molecular simulations on realistic structures. Another way to model the size dependency is using higher order continuum mechanics theories such as strain gradient theory, couple stress theory and nonlocal theory. Because of low computations and modeling accuracy, these theories are used by several researchers to model microtubules in recent years. The researcher's results indicate that applying the nonlocal theory will cause softening of mechanical properties of nano structure while applying the strain gradient or couple stress theories will cause hardening of mechanical properties. Prediction of softening and hardening properties in microtubules also is established by Refs [19,30]. On the other hand, microtubules have actually orthotropic properties; then, applying the strain gradient or couple stress theories for orthotropic material is difficult which can be done as a new research avenue. According to the above discussion, in order to achieve a model that have both properties of high-order continuum theories (softening and hardening) and capability of modeling orthotropic microtubules, in this paper, stress and strain gradient elasticity theory is used. In addition, according to the reference

[31], the advantages of stress and strain gradient elasticity, compared to classical elasticity, are threefold: (i) with gradient elasticity the singularities can be avoided that typically appear in classical elasticity, (ii) the size-dependent mechanical response of heterogeneous materials can be captured with gradient elasticity, and (iii) dispersive wave propagation can be described by gradient elasticity.

As mentioned, microtubules have a cylindrical shell shape and non-isotropic properties. Besides, they are in the nano-scale. Yet, in modeling, it seems that researchers so far have paid attention to one of the three geometrical, mechanical and nano-scale properties of microtubules, or have simultaneously investigated two properties. In this study, however, using cylindrical shell model, a more efficient modeling of microtubule is presented. Moreover, by taking into consideration the orthotropic property, the mechanical behavior of microtubules is more precisely modeled. Finally, using stress and strain gradient elasticity theory, nano-scale behavior and size effects are modeled.

Hence, in this paper, to juxtapose effective parameters of the higher order theory, cylindrical shell model and orthotropic case, the effect of parameters of small size and microtubule dimensions on protein microtubule vibration is investigated based on gradient elasticity theory.

2 PRELIMINARIES

2.1 Orthotropic shell model

In order to investigate the mechanical behavior of microtubules, we need a mathematical model to define the displacement field. Regarding how to choose the model, this model must have acceptable geometrical similarity to the structure under study. Considering the long cylindrical structure of the microtubule, this structure is commonly modeled using beam models or cylindrical shell models.

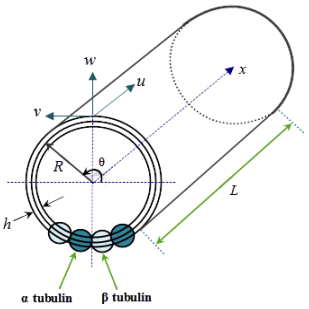

Fig.1
Cylindrical shell model and its variables in microtubule.

The cylindrical shell model (Fig. 1) is fully compatible with the microtubule structure and investigates more details. Besides, experiments have revealed that microtubules are structures with considerable rigidity along length and can be readily categorized as orthotropic structures [32].

In the orthotropic case, 9 independent material parameters (including 3 Young moduli, 3 shear moduli and three Poisson's coefficients) are required to define the mechanical properties in three main directions. In this research, assumptions of plate stress and thin shell reduced the 9 parameters to 4 independent parameters (E_x, E_θ, $G_{x\theta}$ and $\upsilon_{x\theta}$). In different studies, different values have been offered for mechanical properties of microtubules in isotropic and orthotropic cases. Table 1. displays the amount of common properties used.

Table 1
Orthotropic material constants for microtubules [17].

Parameters		Values
Longitudinal modulus [32,33,34]	E_x	0.5~2 GPa
Circumferential modulus [32]	E_θ	1~4 MPa
Shear modulus of microtubules [32,33]	$G_{x\theta}$	1kPa ~1MPa
Poisson's ratio in axial direction [32,34]	$\upsilon_{x\theta}$	0.3
Poisson's ratio in circumferential direction [17]	$\upsilon_{\theta x}$	0.0003
Equivalent thickness [33,34]	h	2.7 nm
Effective thickness for bending [33]	h_0	1.6 nm
Medium radius of microtubule [17]	R	12.8 nm
Mass density per unit volume [34]	ρ	1470 kg/m^3

2.2 Stress and strain gradient elasticity theory

Stress and strain gradient elasticity theory is a combination of Eringen's stress gradient theory and strain gradient theory. This theory includes two size parameters, and strain and structural equations are written as [35]:

$$U = \frac{1}{2}\int_{\forall} \sigma_{ij}\,\varepsilon_{ij}\,d\forall \tag{1}$$

$$(1-l_d^2\,\nabla^2)\sigma_{ij} = C_{ijkl}\,(1-l_s^2\nabla^2)\varepsilon_{kl} \tag{2}$$

where l_s is the size parameter for the static case and l_d is the size parameter for the dynamic case. Also, σ_{ij} and ε_{kl} represent the components of stress and strain respectively, C_{ijkl} represents elements of material stiffness matrix, and ∇^2 represents the Laplace operator. In general, the size parameters mentioned are not equal; rather, their values depend on the size of the representative volume element (RVE) in static and dynamic cases [36,37]. If l_d=0, this theory is reduced to a special form of Mindlin's strain gradient theory, and if l_s=0, it is reduced to Eringen's stress gradient theory. Moreover, by setting both size parameters to zero, this theory converts into the classical theory. In this study, given the fact that the orthotropic shell model is considered, and by considering the assumption of plane stress, ε_{kl} ,C_{ijkl} and ∇^2 are defined as follows:

$$\varepsilon_{kl} = \frac{1}{2}\left(\partial_k u_l + \partial_l u_k\right) \tag{3}$$

$$\nabla^2 = \partial_i^2 + \partial_j^2 + \partial_k^2 \tag{4}$$

$$C_{ijkl} = \begin{bmatrix} \dfrac{E_x}{1-\upsilon_{x\theta}\upsilon_{\theta x}} & \dfrac{E_x\,\upsilon_{\theta x}}{1-\upsilon_{\theta x}\,\upsilon_{x\theta}} & 0 \\ \dfrac{E_\theta \upsilon_{x\theta}}{1-\upsilon_{x\theta}\,\upsilon_{\theta x}} & \dfrac{E_\theta}{1-\upsilon_{x\theta}\upsilon_{\theta x}} & 0 \\ 0 & 0 & 2G_{x\theta} \end{bmatrix} \tag{5}$$

The key issue for successful application of the higher order continuum mechanics models to MTs is to determine the magnitude of the small scale parameter. Due to the stress and strain gradient elasticity theory used in this article which is the combination of high-order continuum models, determining the magnitude of the small scale parameter in nonlocal, strain gradient and couple stress theories is explained here.

In nonlocal theory, in most studies, small scale parameter is usually taken to be 0.39, as proposed by Eringen [12]. For a single walled carbon nanotube, the small scale parameter is found to be less than 2.0 nm [38]. However, there are no experiments conducted to determine the value of the small scale parameter for MTs. Small scale effect on the linear vibration of MTs was carried out analytically by assuming a range of its value since its actual value is not known [39,40]. It has been shown [41,42] that the small scale parameter is different for different physical problems investigated. However, atomistic approach and experimental can be used to determine the small scale parameter in the nonlocal theory.

For strain gradient and couple stress theories, a simple practical and physical interpretation of the length scale parameter can be obtained in term of elastic rigidity of cantilever nanobeam in bending test. Based on modified couple stress theory and considering Euler beam model, the material length scale parameter can be directly related to the difference between the elastic modulus of material [43]. The material length scale parameters also might be determined via molecular dynamic simulation or experiments. Previous researchers used atomistic simulations and molecular dynamics to determine the size effect parameters [44-46]. Maranganti and Sharma [44] used an atomistic

approach to determine strain gradient elasticity constants of structures. They present mathematical derivations that relate the strain-gradient material constants to atomic displacement correlations in a molecular dynamics computational ensemble. Moreover, these parameters can also be determined using mechanical tests [44]. Lam et al. [24] have conducted bending test to determine the strain gradient elastic size parameter of epoxy polymer. Potential experimental errors were determined to be small relative to the observed increase in material rigidity. As mentioned above, several methods such as elastic rigidity of cantilever nanobeam, atomistic approach and experimental were used to determine the microscale parameters in strain gradient and couple stress theories.

3 GOVERNING EQUATIONS OF MICROTUBULE

Fig. 1 displays a schematic form of the cylindrical shell model, where displacement vectors u, v, and w are respectively along orthogonal axes x, θ, and z, which represent length, circumference and radius (perpendicular to the middle plate, and outward). Values of displacement of a given node in the cylindrical shell can be expressed based on Love's thin-shell theory as:

$$\begin{aligned} u(x,\theta,z,t) &= u_0(\mathrm{x},\theta,\mathrm{t}) - z\,\frac{\partial w_0}{\partial x} \\ v(x,\theta,z,t) &= v_0(x,\theta,t) - \frac{z}{R}\left(\frac{\partial w_0}{\partial \theta} - v_0\right) \qquad , \quad w = w_0(x,\theta,t) \end{aligned} \tag{6}$$

where $u_0(\mathrm{x},\theta,\mathrm{t}), v_0(x,\theta,t)$ and $w_0(x,\theta,t)$ represent displacements of the middle plate of the shell.

Considering Eq. (3) and the definitions of displacement vectors and coordinate axes, classical strains are determined as follows:

$$\begin{aligned} &\varepsilon_{zz} = \frac{\partial w}{\partial z} \quad , \quad \varepsilon_{\theta\theta} = \frac{1}{R(1+\frac{z}{R})}\left[\frac{\partial v}{\partial \theta} + w\right] \quad , \quad \varepsilon_{xx} = \frac{\partial u}{\partial x} \\ &\varepsilon_{xz} = \varepsilon_{zx} = \frac{1}{2}\left[\frac{\partial w}{\partial x} + \frac{\partial u}{\partial z}\right] \quad , \quad \varepsilon_{x\theta} = \varepsilon_{\theta x} = \frac{1}{2}\left[\frac{\partial v}{\partial x} + \frac{1}{R(1+\frac{z}{R})}\frac{\partial u}{\partial \theta}\right] \\ &\varepsilon_{\theta z} = \varepsilon_{z\theta} = \frac{1}{2}\left[\frac{1}{R(1+\frac{z}{R})}\frac{\partial w}{\partial \theta} + \frac{\partial v}{\partial z} - \frac{v}{R(1+\frac{z}{R})}\right] \end{aligned} \tag{7}$$

By substituting Eq. (6) into Eq. (7) and considering the assumption of Love's thin shell $\left((1+\frac{z}{R})\approx 1\right)$ non-zero strain components are determined as:

$$\begin{aligned} &\varepsilon_{xx} = \frac{\partial u_0}{\partial x} - z\,\frac{\partial^2 w_0}{\partial x^2} \quad , \quad \varepsilon_{\theta\theta} = \frac{1}{R}\frac{\partial v_0}{\partial \theta} + \frac{w_0}{R} - \frac{z}{R^2}\frac{\partial^2 w_0}{\partial \theta^2} \\ &\varepsilon_{x\theta} = \varepsilon_{\theta x} = \frac{1}{2}\left[\frac{1}{R}\frac{\partial u_0}{\partial \theta} + \frac{\partial v_0}{\partial x} - \frac{2z}{R}\,\frac{\partial^2 w_0}{\partial x\,\partial \theta}\right] \end{aligned} \tag{8}$$

By substituting the strains obtained into Eq. (1), and multiplying its two sides by $(1-l_d^2\nabla^2)$ the following is resulted:

$$(1-l_d^2\nabla^2)U=(1-l_d^2\nabla^2)\int_\theta\int_x\left\{\int_{-\frac{h}{2}}^{\frac{h}{2}}\left[\sigma_x\frac{\partial u_0}{\partial x}-\sigma_x z\frac{\partial^2 w_0}{\partial x^2}+\sigma_\theta\frac{\partial v_0}{R\partial\theta}+\sigma_\theta\frac{w_0}{R}-\right.\right.$$
$$\left.\left.\sigma_\theta z\frac{\partial^2 w_0}{R^2\partial\theta^2}+\sigma_{x\theta}\frac{\partial u_0}{R\partial\theta}+\sigma_{x\theta}\frac{\partial v_0}{\partial x}-2\sigma_{x\theta}z\frac{\partial^2 w_0}{R\partial x\partial\theta}\right]dz\right\}Rdxd\theta \tag{9}$$

Now, by defining classical force and torques (see Appendix A for more details),

$$\{N_x,N_\theta,N_{x\theta}\}=\int_{-\frac{h}{2}}^{\frac{h}{2}}\{\sigma_x,\sigma_\theta,\sigma_{x\theta}\}dz \tag{10}$$

$$\{M_x,\mathrm{M}_\theta,M_{x\theta}\}=\int_{-\frac{h}{2}}^{\frac{h}{2}}\{\sigma_x,\sigma_\theta,\sigma_{x\theta}\}zdz \tag{11}$$

Strain energy of cylindrical thin shell in Eq. (9) is determined as:

$$A_1U=\int_\theta\int_x A_1\left[N_x\frac{\partial u_0}{\partial x}-M_x\frac{\partial^2 w_0}{\partial x^2}+N_\theta\left(\frac{\partial v_0}{R\partial\theta}+\frac{w_0}{R}\right)-M_\theta\frac{\partial^2 w_0}{R^2\partial\theta^2}+\right.$$
$$\left.N_{x\theta}\left(\frac{\partial u_0}{R\partial\theta}+\frac{\partial v_0}{\partial x}\right)-2M_{x\theta}\frac{\partial^2 w_0}{R\partial x\partial\theta}\right]Rdxd\theta \tag{12}$$

which is $\mathrm{A}_1=(1-l_d^2\nabla^2)$ in Eq. (12) and kinetic energy, in general, is expressed as:

$$\mathrm{T}=\frac{1}{2}\rho\int_V(\dot{u}^2+\dot{v}^2+\dot{w}^2)dV \tag{13}$$

Now, by substituting the components of displacement from Eq. (6) into (13), the kinetic energy of cylindrical shell is expressed as:

$$\mathrm{T}=\frac{1}{2}\rho\int_\theta\int_x\left\{\int_{-\frac{h}{2}}^{\frac{h}{2}}\left[\left(\frac{\partial u_0}{\partial t}-z\frac{\partial^2 w_0}{\partial x\partial t}\right)^2+\left(\frac{\partial v_0}{\partial t}-\frac{z}{R}\frac{\partial^2 w_0}{\partial\theta\partial t}\right)^2+\left(\frac{\partial w_0}{\partial t}\right)^2\right]dz\right\}Rdxd\theta \tag{14}$$

The work of external forces acting on the cylindrical shell is expressed as:

$$W=\int_\theta\int_x\left(f_x u_0+f_\theta v_0+f_z w_0\right)Rdxd\theta \tag{15}$$

Now, by considering Hamilton's principle as follows, one can derive the governing equations of the microtubule.

$$\int_{t_1}^{t_2}\left(\delta T+\delta W-\delta U\right)dt=0 \tag{16}$$

By multiplying $(1-l_d^2\nabla^2)$ by Eq. (16) and then performing substitution and variation for Eqs. (12), (14) and (15), and finally integrating and setting coefficients $\delta u_0,\delta v_o$ and δw_0 to zero (see Appendix A for more details),

equations of motion and boundary conditions of the orthotropic cylindrical shell are derived based on the stress-strain gradient elasticity theory as:

$$A_2\left[a_1\frac{\partial^2 u_0}{\partial x^2}+a_2\left(\frac{\partial^2 v_0}{\partial\theta\partial x}+\frac{\partial w_0}{\partial x}\right)+a_3\frac{\partial^2 u_0}{\partial\theta^2}+a_4\frac{\partial^2 v_0}{\partial x\,\partial\theta}\right]=A_1\left(\rho Rh\frac{\partial^2 u_0}{\partial t^2}\right)-A_1Rf_x \tag{17}$$

$$A_2\left[b_1\frac{\partial^2 u_0}{\partial x\,\partial\theta}+b_2\left(\frac{\partial^2 v_0}{\partial\theta^2}+\frac{\partial w_0}{\partial\theta}\right)+b_3\frac{\partial^2 u_0}{\partial\theta\partial x}+b_4\frac{\partial^2 v_0}{\partial x^2}\right]=A_1\left(\rho Rh\frac{\partial^2 v_0}{\partial t^2}\right)-A_1Rf_\theta \tag{18}$$

$$\begin{aligned}&A_2\left[c_1\frac{\partial^4 w_0}{\partial x^4}+c_2\frac{\partial^4 w_0}{\partial x^2\partial\theta^2}+c_3\frac{\partial^4 w_0}{\partial x^2\partial\theta^2}+c_4\frac{\partial^4 w_0}{\partial\theta^4}+c_5\frac{\partial^4 w_0}{\partial x^2\partial\theta^2}+c_6\frac{\partial u_0}{\partial x}+\right.\\&\left.c_7\left(\frac{\partial v_0}{\partial\theta}+w_0\right)\right]=A_1\left(\frac{\rho Rh^3}{12}\frac{\partial^4 w_0}{\partial x^2\partial t^2}+\frac{\rho h^3}{12R}\frac{\partial^4 w_0}{\partial\theta^2\partial t^2}-\rho hR\frac{\partial^2 w_0}{\partial t^2}\right)+A_1Rf_z\end{aligned} \tag{19}$$

Boundary conditions for the edge with constant x coefficient are as follows:

$$\int_\theta \mathrm{A}_2\left[a_1\frac{\partial u_0}{\partial x}+a_2\left(\frac{\partial v_0}{\partial\theta}+\mathrm{w}_0\right)\right]d\theta\Big|_{x=0,L}=0 \qquad or \qquad \delta u_0\big|_{x=0,L}=0 \tag{20}$$

$$\int_\theta \mathrm{A}_2\left[a_3\frac{\partial u_0}{\partial\theta}+a_4\frac{\partial v_0}{\partial x}\right]d\theta\Big|_{x=0,L}=0 \qquad or \qquad \delta v_0\big|_{x=0,L}=0 \tag{21}$$

$$\int_\theta \mathrm{A}_2\left[c_1\frac{\partial^2 w_0}{\partial x^2}+c_2\frac{\partial^2 w_0}{\partial\theta^2}\right]d\theta\Big|_{x=0,L}=0 \qquad or \qquad \delta\left(\frac{\partial w_0}{\partial x}\right)\Big|_{x=0,L}=0 \tag{22}$$

$$\int_\theta \mathrm{A}_2\left[c_1\frac{\partial^3 w_0}{\partial x^3}+c_2\frac{\partial^3 w_0}{\partial x\,\partial\theta^2}+c_5\frac{\partial^3 w_0}{\partial x\,\partial\theta^2}\right]d\theta\Big|_{x=0,L}=0 \qquad or \qquad \delta w_0\big|_{x=0,L}=0 \tag{23}$$

Boundary conditions for the edge with constant θ coefficient are as follows:

$$\int_x \mathrm{A}_2\left[a_3\frac{\partial u_0}{\partial\theta}+a_4\frac{\partial v_0}{\partial x}\right]dx\,\Big|_{\theta=0,\theta_0}=0 \qquad or \qquad \delta u_0\big|_{\theta=0,\theta_0}=0 \tag{24}$$

$$\int_x \mathrm{A}_2\left[b_1\frac{\partial u_0}{\partial x}+b_2\left(\frac{\partial v_0}{\partial\theta}+w_0\right)\right]dx\,\Big|_{\theta=0,\theta_0}=0 \qquad or \qquad \delta v_0\big|_{\theta=0,\theta_0}=0 \tag{25}$$

$$\int_x \mathrm{A}_2\left[c_3\frac{\partial^2 w_0}{\partial x^2}+c_4\frac{\partial^2 w_0}{\partial\theta^2}\right]dx\,\Big|_{\theta=0,\theta_0}=0 \qquad or \qquad \delta\left(\frac{\partial w_0}{\partial\theta}\right)\Big|_{\theta=0,\theta_0}=0 \tag{26}$$

$$\int_x \mathrm{A}_2\left[c_3\frac{\partial^3 w_0}{\partial x^2\partial\theta}+c_4\frac{\partial^3 w_0}{\partial\theta^3}+c_5\frac{\partial^3 w_0}{\partial x^2\partial\theta}\right]dx\,\Big|_{\theta=0,\theta_0}=0 \qquad or \qquad \delta w_0\big|_{\theta=0,\theta_0}=0 \tag{27}$$

4 FORMULATING AND SOLVING EQUATIONS FOR THE SPECIAL CASE

In this section, to evaluate the new equations of motion derived from the theory and model used, the circular cylindrical shell with simply supported boundary conditions is generalized. For the simple support at the two edges of the cylindrical shell, boundary conditions in Eqs. (24) and (27) are existent due to the variability of θ. Therefore, boundary conditions in Eqs. (20)-(23) must be satisfied. For this purpose, the main boundary conditions in the simple support are as follows:

$$\begin{aligned} v_0\big|_{x=0,L} &= 0 \\ w_0\big|_{x=0,L} &= 0 \end{aligned} \tag{28}$$

Besides, by rewriting natural boundary conditions resulting from the freedom of the two ends of the nanoshell from bending moment, the final natural boundary conditions for the simply supported circular cylindrical shell are as follows:

$$\int_\theta \mathrm{A}_2 \left[a_1 \frac{\partial u_0}{\partial x} + a_2 \left(\frac{\partial v_0}{\partial \theta} + w_0 \right) \right] d\theta \big|_{x=0,L} = 0 \tag{29}$$

$$\int_\theta \mathrm{A}_2 \left[c_1 \frac{\partial^2 w_0}{\partial x^2} + c_2 \frac{\partial^2 w_0}{\partial \theta^2} \right] d\theta \big|_{x=0,L} = 0 \tag{30}$$

Now, to solve the free vibration of the protein microtubule, one must solve Eqs. (17)-(19) as well as boundary conditions in Eqs. (28)-(30). In so doing, and to solve equations of motion and boundary conditions, displacements are used with the aid of the Navier method as follows:

$$\begin{cases} u_0 = \sum_{m=1}^{\infty} \sum_{n=1}^{\infty} U_{mn} \cos\left(\frac{m\pi}{L} x \right) \sin(n\theta) e^{i\omega t} \\ v_0 = \sum_{m=1}^{\infty} \sum_{n=1}^{\infty} V_{mn} \sin\left(\frac{m\pi}{L} x \right) \cos(n\theta) e^{i\omega t} \\ w_0 = \sum_{m=1}^{\infty} \sum_{n=1}^{\infty} W_{mn} \sin\left(\frac{m\pi}{L} x \right) \sin(n\theta) e^{i\omega t} \end{cases} \tag{31}$$

where U_{mn}, V_{mn} and W_{mn} represent amplitude of vibration along length, circumference and radius. Also, m and n are axial wave number and circumferential wave number, respectively.

Considering the displacements assumed in Eq. (31), it is clear that all boundary conditions in Eqs. (28)-(30) are satisfied. Now, to solve the free vibration of the microtubule, one must simply solve equations of motion (17)-(19). In so doing, displacements are substituted from Eq. (31) into Eqs. (17)-(19) and rewritten in the matrix form as follows (See Appendix B for more details):

$$\left[K - \omega^2 M \right] \{d_0\} = 0 \tag{32}$$

where $\{d_0\}^T = \{U_{mn} \quad V_{mn} \quad W_{mn}\}$ and ω represent natural frequency. To derive non-trivial solutions from Eq. (32), the determinant of the coefficients matrix must be zero.

5 RESULTS AND INVESTIGATIONS

In this section, by assigning values to variables and parameters existing in equations derived in the last section and final solution of equations, the solutions are displayed numerically and graphically. Besides, the effect of different factors such as size parameter, geometrical parameters and mechanical properties on microtubule vibration is investigated. Table 1. displays the values of mechanical properties of the microtubule, and the dimensionless natural frequency is defined as $\Omega = R\omega\sqrt{\rho(1-\upsilon_{x\theta}\upsilon_{\theta x})/E_x}$.

5.1 Comparing results with the references

Considering the fact that the formulation presented in this paper is being used for the microtubule for the first time, the results could not be investigated except in special cases. In order to evaluate the results, considering that the results exist in the classical case, one can compare the results in the classic case with other studies. As mentioned in previous sections, by setting both size parameters to zero, the stress-strain gradient theory is reduced to the classical theory. Different papers have offered different values for the mechanical properties of the microtubule. In the results of other studies mentioned in Table 2. , except the common values $R=10.7nm$, $h=1.6nm$, $\upsilon=0.3$, material properties are assumed to be $E_x=129\ MPa$, $E_\theta=1.02MPa$ and $G_{x\theta}=1.4MPa$ in Shen [19]; $E_x=1GPa$, $E_\theta=1MPa$, and $G_{x\theta}=0.01MPa$ in Shi et al. [47]; $E_x=1.32GPa$, $E_\theta=4MPa$ and $G_{x\theta}=0.01MPa$ in Tuszynski et al. [32]; and isotropic material properties are assumed to be $E=0.8GPa$ and $G=E/2(1+\upsilon)$ in de Pablo et al. [33]. To draw a better comparison, results of this study are in turn solved with each of the values in the above references. Table 2. displays the existing results and the results of each reference.

We know that the theory used in this article can be converted on the particular mode to the nonlocal theory. Therefore, in Table 2. , the comparison between the results of this work and reference [19] has been completed. It should be noted that, in this paper, l_s=0 is considered and also in reference [19] the nonlocal theory is used. By comparing the results of Table 2. , it can be understood that although the theory used in both articles is equal, the results are different. This difference is due to Reddy's higher order shear deformation shell theory and the Kármán-Donnell-type nonlinear motion used in reference [19], but thin shell model with linear motion is used in this paper.

Table 2
Comparing the frequency (GHz) of microtubule modeled with classical and nonclassical cylindrical shell to other works

Source	*L*/*R*		
	100	300	500
Shen [19] (l_s=e_0a=0)	-	0.1063	0.1063
Present work(l_s=l_s=0)	0.1007	0.0757	0.0752
Shen [19] (l_s=e_0a=3.85 nm)	-	0.1	0.1
Present work(l_s=0, l_s=3.85 nm)	-	0.0751	0.0751
Shi et al. [47]	0.0955	0.0952	0.0952
Present work	0.0758	0.0745	0.0744
Tuszynski et al. [32]	0.1535	0.1533	0.1533
Present work	0.1496	0.1488	0.1487
de Pablo et al. [33]	3.1131	3.1097	3.1095

By comparing the results, it becomes clear that the isotropic case predicts the frequency to be higher than the orthotropic case, and this difference is partially due to the dependence of shear modulus and lateral elasticity modulus on longitudinal elasticity modulus, and, as a result, their results are much higher than the real amount in the isotropic case for the microtubule. It is also demonstrated that the results of the present study predict the frequency to be slightly lower than the references do, one reason of which could be the assumption of thin shell. Another point worth noting is the decrease in frequency due to increase in microtubule length (the effect of which decreases in greater lengths). Of course, it should be noted that the theory used in Shen [19] is the nonlocal theory and hence the difference in results. In Shi et al. [47], the beam model is used and therefore, difference could still be seen. However, with a geometrically similar model, the results of this study have appropriate consistency with Tuszynski et al. [32]. Finally, in de Pablo et al. [33], because of the use of isotropic behavior, the difference in the results is high.

5.2 Effect of mechanical properties of microtubule on frequency

As displayed in Table 1. , some of microtubule mechanical properties such as E_x, E_θ, and $G_{x\theta}$ lack a fixed value, and values assigned to them are sometimes in a broad range. In this section, by separately investigating each of these properties and keeping other parameters constant, their effect on the first natural frequency is graphically modeled. It should be noted that, except for the three investigated parameters, values displayed in Table 1. as well as $L=1e\text{-}6m$, $n=2$, $l_d=3nm$, $l_s=10nm$ and $k=m\pi/L$ are taken into consideration in this section.

It is predicted that in vibration systems, natural frequency has a direct relationship to system stiffness, and this can be seen in Figs. 2 and 3.

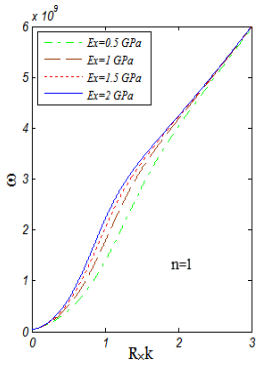

Fig.2
Effect of E_x variation on natural frequency of microtubule ($E_\theta=1MPa$, $G_{x\theta}=0.1MPa$).

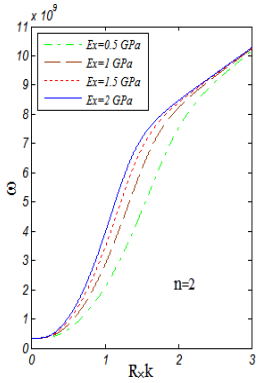

Fig.3
Effect of E_x variation on natural frequency of microtubule ($E_\theta=1MPa$, $G_{x\theta}=0.1MPa$).

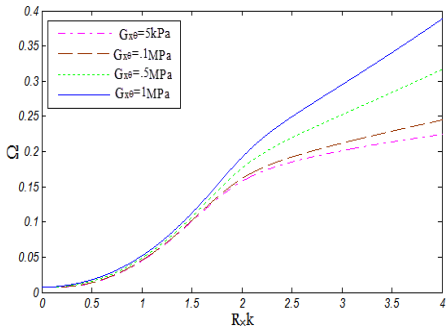

Fig.4
Effect of $G_{x\theta}$ variation on dimensionless frequency of microtubule ($E_x=1Gpa$, $E_\theta=2MPa$).

Figs. 2 and 3 demonstrate that increase in E_x , and consequently increase in microtubule stiffness leads to increase in natural frequency. Yet, because of the dominance of the effect of L, in both cases of great axial

wavelengths $(R \times k \leq 0.3)$ and small axial wave lengths $(R \times k \geq 2.5)$, the effect of variation E_x is infinitesimal. In fact, the greatest effect is in the $0.1 \leq mR/L \leq 0.8$ interval. Also, in addition to the increase in frequency induced by decrease in axial wavelengths (decrease in L or increase in m in $m\pi R/L$ equation), comparison of Figs. 2 and 3 reveals that increase in n increases frequency too.

Considering that components of matrix K are dependent on the values of E_θ and $G_{x\theta}$, increase in these two moduli, too, increases natural frequency of microtubule. Figs. 4 and 5 display these changes. However, the noteworthy point is that, unlike E_x, the diagrams are not convergent in small axial wavelengths for these two moduli. By having another look at the elements of variation matrix in Appendix B, one can see some exponents of $m\pi/L$ and n as coefficients for elasticity moduli E_x, E_θ, and $G_{x\theta}$. Another important point is the dependence of E_x on the size of axial wavelength considering the presence of a non-zero exponent of $m\pi/L$ along with E_x besides its presence in other elements, while this dependency does not exist for E_θ and $G_{x\theta}$.

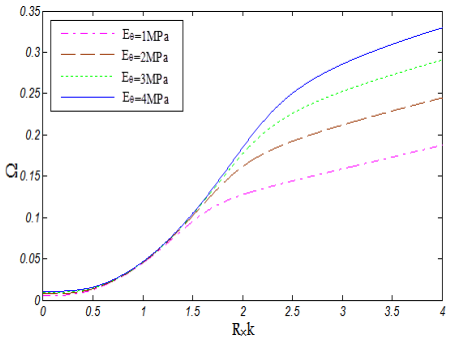

Fig.5
Effect of E_θ variation on dimensionless natural frequency of microtubule (E_x=*1Gpa*, $G_{x\theta}$=*0.1MPa*).

5.3 Effect of size parameters on frequency

As mentioned in Section 2, size parameters l_s and l_d are dependent on the dimensions of the element under investigation in this study. Considering the variation of length, and, to some extent, radius of the microtubule, the value of size parameters is variable too. Table 3. and Table 4. display the effect of these parameters in different lengths on the natural frequency of microtubule.

The results of these tables could be divided into four sections based on the values of l_s and l_d for each microtubule length. The results of the first section are related to the classical frequency and include the first three rows of the first column in each microtubule length $(l_s = l_d = 0)$. The second section includes the frequencies of the first column except its first three rows, and is related to a special form of stress gradient theory ($l_s = 0$). The third section includes the frequencies of the first three rows except the first column, and is related to stress gradient theory ($l_s = 0$). The fourth section includes the results relating to the intended theory in this study and frequencies obtained for non-zero values of l_s and l_d.

Comparison of the results of decrease in frequency values induced by increase in l_d and increase in frequency values induced by increase in l_s makes it clear that the results are inclined toward the prediction of results by the nonlocal theory in the first case and the strain gradient theory in the second. And according to the results predicted in the references, it is for the effect of softening in the nonlocal theory and the effect of stiffening in the strain gradient theory. In other words, the stress-strain gradient theory used in this paper is capable of combining the advantages of the two nonlocal and strain gradient theories and can eliminate the drawbacks of these two theories. Hence it is a more comprehensive theory.

Increase in microtubule length, besides having a general effect on frequency, leads to different intensity decreases for each frequency modes. For the first frequency, the intensity of frequency decrease in the nano scale undergoes a considerable decrease. In the micro scale, however, this intensity is mild and approaches stability. The slope of decrease for the second frequency is average and almost steady. The intensity of increase of the third frequency is high in the beginning, and then becomes average, and in the end it becomes very mild. It should be noted that E_x=*1GPa* ،E_θ=*1MPa* ،$G_{x\theta}$=*0.1MPa* ،*n=2* and *m=4* are assumed.

Table 3
Effect of size parameters on microtubule natural frequency.

		l_d(nm)							
l_s	natural frequency	L=100 nm				L=1 μm			
(nm)	(GHz)	0	1	3	6	0	1	3	6
0	ω_1	3.520	3.450	3.015	2.249	0.2110	0.2090	0.1910	0.1538
	ω_2	5.510	5.400	4.723	3.523	4.5520	4.4970	4.1180	3.3155
	ω_3	103.66	101.64	88.826	66.260	10.445	10.319	9.4520	7.6085
5	ω_1	4.980	4.880	4.270	3.185	0.2680	0.2650	0.2430	0.1954
	ω_2	7.800	7.650	6.690	4.989	5.8730	5.7130	5.2330	4.2125
	ω_3	146.78	143.92	125.78	93.826	13.271	13.111	12.009	9.6670
10	ω_1	7.880	7.730	6.7600	5.040	0.3930	0.3880	0.3550	0.2860
	ω_2	12.350	12.110	10.580	7.890	8.4630	8.3610	7.6580	6.1650
	ω_3	232.26	227.73	199.03	148.47	10.527	19.187	17.575	14.147
20	ω_1	14.540	14.260	12.460	9.300	0.6950	0.6860	0.6290	0.5060
	ω_2	22.780	22.330	19.520	14.560	14.978	14.797	13.554	10.910
	ω_3	428.43	420.06	367.12	273.86	34.327	33.957	31.104	25.037
30	ω_1	21.450	21.040	18.380	13.710	1.0150	1.0030	0.9180	0.7390
	ω_2	33.610	32.950	28.800	21.480	21.883	21.619	19.802	15.940
	ω_3	632.10	619.77	541.66	404.05	50.217	49.612	45.443	36.580

Table 4
Effect of size parameters on microtubule natural frequency.

		l_d(nm)							
l_s	natural frequency	L=4 μm				L=10 μm			
(nm)	(GHz)	0	1	3	6	0	1	3	6
0	ω_1	0.2016	0.1992	0.1825	0.1471	0.2013	0.1989	0.1823	0.1469
	ω_2	2.8938	2.8591	2.6201	2.1109	1.6538	1.6340	1.4974	1.2065
	ω_3	4.5512	4.4966	4.1208	3.3200	4.5510	4.4965	4.1207	3.3201
5	ω_1	0.2558	0.2528	0.2316	0.1866	0.2555	0.2524	0.2313	0.1864
	ω_2	3.6725	3.6284	3.3251	2.6789	2.0987	2.0735	1.9002	1.5310
	ω_3	5.7759	5.7067	5.2297	4.2134	5.7753	5.7060	5.2293	4.2132
10	ω_1	0.3740	0.3695	0.3387	0.2728	0.3734	0.3690	0.3381	0.2724
	ω_2	5.3690	5.3046	4.8612	3.9165	3.0680	3.0312	2.7779	2.2382
	ω_3	8.4442	8.3429	7.6456	6.1598	8.4428	8.3416	7.6446	6.1592
20	ω_1	0.6620	0.6540	0.5990	0.4830	0.6610	0.6530	0.5980	0.4820
	ω_2	9.4960	9.3830	8.5980	6.9270	5.4260	5.3610	4.9130	3.9590
	ω_3	14.936	14.757	13.523	10.895	14.933	14.754	13.521	10.894
30	ω_1	0.9660	0.9550	0.8750	0.7050	0.9650	0.9530	0.8740	0.7040
	ω_2	13.872	13.706	12.560	10.119	7.9270	7.8320	7.1770	5.7830
	ω_3	21.818	21.556	19.755	15.916	21.814	21.552	19.751	15.914

6 CONCLUSIONS

In this study, by considering size parameters in stress - strain gradient elasticity theory and using orthotropic cylindrical shell model and the assumption of thin shell, a new formulation was developed for investigating the vibration of protein microtubule, and the analytical solution of equations for the simply supported case was obtained. By setting both size parameters to zero, the results in the classic case were compared with other results and the formulation was verified. Afterwards, the effect of different mechanical properties was investigated, demonstrating that increase in elasticity moduli E_x, E_θ and $G_{x\theta}$ and decrease in axial wavelength lead to increase in the natural frequency of microtubule. In the end, the effect of different values of size parameters on the natural frequency of microtubule was investigated, yielding the conclusion that frequencies decrease with the increase in l_d and increase with the increase in l_s.

APPENDIX A

By substituting Eqs. (8) and (5) into (2) and then substituting the result into Eqs. (10) and (11), the classical forces and torques are determined as:

$$(1-l_d^2\nabla^2)N_x=(1-l_s^2\nabla^2)\mathrm{h}\left[\mathrm{C}_{11}\frac{\partial u_0}{\partial x}+\frac{C_{12}}{R}\left(\frac{\partial v_0}{\partial\theta}+w_0\right)\right] \tag{A.1}$$

$$(1-l_d^2\nabla^2)N_\theta=(1-l_s^2\nabla^2)\mathrm{h}\left[\mathrm{C}_{21}\frac{\partial u_0}{\partial x}+\frac{C_{22}}{R}\left(\frac{\partial v_0}{\partial\theta}+w_0\right)\right] \tag{A.2}$$

$$(1-l_d^2\nabla^2)N_{x\theta}=(1-l_s^2\nabla^2)\mathrm{G}_{x\theta}\mathrm{h}\left[\frac{1}{R}\frac{\partial u_0}{\partial\theta}+\frac{\partial v_0}{\partial x}\right] \tag{A.3}$$

$$(1-l_d^2\nabla^2)M_x=(1-l_s^2\nabla^2)\frac{h^3}{12}\left[-C_{11}\frac{\partial^2 w_0}{\partial x^2}-\frac{C_{12}}{R^2}\frac{\partial w_0}{\partial\theta^2}\right] \tag{A.4}$$

$$(1-l_d^2\nabla^2)M_\theta=(1-l_s^2\nabla^2)\frac{h^3}{12}\left[-C_{21}\frac{\partial^2 w_0}{\partial x^2}-\frac{C_{22}}{R^2}\frac{\partial^2 w_0}{\partial\theta^2}\right] \tag{A.5}$$

$$(1-l_d^2\nabla^2)M_{x\theta}=(1-l_s^2\nabla^2)\frac{G_{x\theta}h^3}{6R}\left[-\frac{\partial^2 w_0}{\partial x\,\partial\theta}\right] \tag{A.6}$$

Strain energy variation from Eq. (1) is as follows:

$$\delta U=\frac{1}{2}\int_{\forall}\sigma_{ij}\delta\varepsilon_{ij}d\forall \tag{A.7}$$

Or, in the extended case, it can be expressed as:

$$\delta U=\int_x\int_\theta\int_{-\frac{h}{2}}^{\frac{h}{2}}\left[\sigma_x\delta\varepsilon_x+\sigma_\theta\delta\varepsilon_\theta+2\sigma_{x\theta}\delta\varepsilon_{x\theta}\right]dz\,(R\,dx\,d\theta) \tag{A.8}$$

By substituting strains from Eq. (8) and multiplying $(1-l_d^2\nabla^2)$ by Eq. (8), one can write:

$$\begin{aligned}\frac{A_1}{(1-l_d^2\nabla^2)}\delta U=(1-l_d^2\nabla^2)\int_\theta\int_x\left\{\int_{-\frac{h}{2}}^{\frac{h}{2}}\left[\sigma_x\frac{\partial(\delta u_0)}{\partial x}-\sigma_x z\frac{\partial^2(\delta w_0)}{\partial x^2}+\sigma_\theta\frac{\partial(\delta v_0)}{R\,\partial\theta}+\right.\right.\\ \left.\left.\sigma_\theta\frac{\delta w_0}{R}-\sigma_\theta z\frac{\partial^2(\delta w_0)}{R^2\partial\theta^2}+\sigma_{x\theta}\frac{\partial(\delta u_0)}{R\,\partial\theta}+\sigma_{x\theta}\frac{\partial(\delta v_0)}{\partial x}-2\sigma_{x\theta}z\frac{\partial^2(\delta w_0)}{R\,\partial x\,\partial\theta}\right]dz\right\}R\,dx\,d\theta\end{aligned} \tag{A.9}$$

The above equation, considering the definition of classical forces and torques can be written as follows:

$$A_1\delta U = \int_\theta\int_x A_1\left[N_x\frac{\partial(\delta u_0)}{\partial x} - M_x\frac{\partial^2(\delta w_0)}{\partial x^2} + N_\theta\left(\frac{\partial(\delta v_0)}{R\,\partial\theta} + \frac{(\delta w_0)}{R}\right) - M_\theta\frac{\partial^2(\delta w)_0}{R^2\partial\theta^2} + N_{x\theta}\left(\frac{\partial(\delta u_0)}{R\,\partial\theta} + \frac{\partial(\delta v_0)}{\partial x}\right) - 2M_{x\theta}\frac{\partial^2(\delta w_0)}{R\,\partial x\,\partial\theta}\right]R\,dx\,d\theta \tag{A.10}$$

Now, by integrating by parts from Eq. (A.10), the following equations are derived:

$$\int_\theta\left\{\int_x A_1N_x\frac{\partial(\delta u_0)}{\partial x}dx\right\}d\theta = \int_\theta\left\{(A_1N_x\,\delta u_0)_0^L - \int_x \delta u_0\frac{\partial(A_1N_x)}{\partial x}dx\right\}d\theta = \int_\theta(A_1N_x\,\delta u_0)_0^L\,d\theta - \int_\theta\int_x \delta u_0\frac{\partial(A_1N_x)}{\partial x}dx\,d\theta \tag{A.11}$$

$$\int_\theta\left\{\int_x M_xA_1\frac{\partial^2(\delta w_0)}{\partial x^2}dx\right\}d\theta = \int_\theta\left\{\left(A_1M_x\frac{\partial(\delta w_0)}{\partial x}\right)_0^L - \int_x\frac{\partial(A_1M_x)}{\partial x}\frac{\partial(\delta w_0)}{\partial x}dx\right\}d\theta = \int_\theta\left(A_1M_x\frac{\partial(\delta w_0)}{\partial x}\right)_0^L d\theta - \int_\theta\left(\delta w_0\frac{\partial(A_1M_x)}{\partial x}\right)_0^L d\theta + \int_\theta\int_x \delta w_0\frac{\partial^2(A_1M_x)}{\partial x^2}dx\,d\theta \tag{A.12}$$

$$\int_x\left\{\int_\theta A_1N_\theta\frac{\partial(\delta v_0)}{\partial\theta}d\theta\right\}dx = \int_x\left\{(A_1N_\theta\delta v_0)_0^{2\pi} - \int_\theta\delta v_0\frac{\partial(A_1N_\theta)}{\partial\theta}d\theta\right\}dx = \int_x(A_1N_\theta\delta v_0)_0^{2\pi}dx - \int_x\int_\theta\delta v_0\frac{\partial(A_1N_\theta)}{\partial\theta}d\theta\,dx \tag{A.13}$$

$$\int_x\left\{\int_\theta A_1M_\theta\frac{\partial^2(\delta w_0)}{\partial\theta^2}d\theta\right\}dx = \int_x\left\{\left(A_1M_\theta\frac{\partial(\delta w_0)}{\partial\theta}\right)_0^{2\pi} - \int_\theta\frac{\partial(A_1M_\theta)}{\partial\theta}\frac{\partial(\delta w_0)}{\partial\theta}d\theta\right\}dx = \int_x\left(A_1M_\theta\frac{\partial(\delta w_0)}{\partial\theta}\right)_0^{2\pi}dx - \int_x\left(\delta w_0\frac{\partial(A_1M_\theta)}{\partial\theta}\right)_0^{2\pi}dx + \int_x\int_\theta\delta w_0\frac{\partial^2(A_1M_\theta)}{\partial\theta^2}dx\,d\theta \tag{A.14}$$

$$\int_x\left\{\int_\theta A_1N_{x\theta}\frac{\partial(\delta u_0)}{\partial\theta}d\theta\right\}dx = \int_x\left\{(A_1N_{x\theta}\delta u_0)_0^{2\pi} - \int_\theta\delta u_0\frac{\partial(A_1N_{x\theta})}{\partial\theta}d\theta\right\}dx = \int_x(A_1N_{x\theta}\delta u_0)_0^{2\pi}dx - \int_x\int_\theta\delta u_0\frac{\partial(A_1N_{x\theta})}{\partial\theta}d\theta\,dx \tag{A.15}$$

$$\int_\theta\left\{\int_x A_1N_{x\theta}\frac{\partial(\delta v_0)}{\partial x}dx\right\}d\theta = \int_\theta\left\{(A_1N_{x\theta}\delta v_0)_\circ^L - \int_x\delta v_0\frac{\partial(A_1N_{x\theta})}{\partial x}dx\right\}d\theta = \int_\theta(A_1N_{x\theta}\delta v_0)_0^L\,d\theta - \int_\theta\int_x\delta v_0\frac{\partial(A_1N_{x\theta})}{\partial x}dx\,d\theta \tag{A.16}$$

$$\int_\theta\left\{\int_x A_1M_{x\theta}\frac{\partial^2(\delta w_0)}{\partial x\,\partial\theta}dx\right\}d\theta = \int_\theta\left\{\left(A_1M_{x\theta}\frac{\partial(\delta w_0)}{\partial\theta}\right)_0^L - \int_x\frac{\partial(A_1M_{x\theta})}{\partial x}\frac{\partial(\delta w_0)}{\partial\theta}dx\right\}d\theta = \int_x\int_\theta\delta w_0\frac{\partial^2(A_1M_{x\theta})}{\partial x\,\partial\theta}d\theta\,dx - \int_\theta\left(\delta\,\mathrm{w}_0\frac{\partial(A_1M_{x\theta})}{\partial\theta}\right)_0^L d\theta - \int_x\left(\delta w_0\frac{\partial(A_1M_{x\theta})}{\partial x}\right)_0^{2\pi}dx + \left[(A_1M_{x\theta}\delta w_0)_0^L\right]_0^{2\pi} \tag{A.17}$$

By substituting Eqs. (A.1)-(A.6) into Eqs. (A.11)-(A.17), strain energy variation and boundary conditions can be written as follows:

$$A_1\delta U = -\int_x\int_\theta A_2\left\{\left[a_1\frac{\partial^2 u_0}{\partial x^2}+a_2\left(\frac{\partial^2 v_0}{\partial x\,\partial\theta}+\frac{\partial w_0}{\partial x}\right)+a_3\frac{\partial^2 u_0}{\partial\theta^2}+a_4\frac{\partial^2 v_0}{\partial x\,\partial\theta}\right]\delta u_0+\right.$$
$$\left[b_1\frac{\partial^2 u_0}{\partial x\,\partial\theta}+b_2\left(\frac{\partial^2 v_0}{\partial\theta^2}+\frac{\partial w_0}{\partial\theta}\right)+b_3\frac{\partial^2 u_0}{\partial\theta\partial x}+b_4\frac{\partial^2 v_0}{\partial x^2}\right]\delta v_0+\left[-c_1\frac{\partial^4 w_0}{\partial x^4}-c_2\frac{\partial^4 w_0}{\partial x^2\partial\theta^2}\right. \quad (A.18)$$
$$\left.\left.-c_3\frac{\partial^4 w_0}{\partial x^2\partial\theta^2}-c_4\frac{\partial^4 w_0}{\partial\theta^4}-c_5\frac{\partial^4 w_0}{\partial x^2\partial\theta^2}-c_6\frac{\partial u_0}{\partial x}-c_7\left(\frac{\partial v_0}{\partial\theta}+w_0\right)\right]\delta w_0\right\}d\theta dx$$

Boundary conditions for the edge with constant x coefficient are as follows:

$$\int_\theta \mathrm{A}_2\left[a_1\frac{\partial u_0}{\partial x}+a_2\left(\frac{\partial v_0}{\partial\theta}+\mathrm{w}_0\right)\right]d\theta\Big|_{x=0,L}=0 \qquad or \qquad \delta u_0\big|_{x=0,L}=0 \quad (A.19)$$

$$\int_\theta \mathrm{A}_2\left[a_3\frac{\partial u_0}{\partial\theta}+a_4\frac{\partial v_0}{\partial x}\right]d\theta\Big|_{x=0,L}=0 \qquad or \qquad \delta v_0\big|_{x=0,L}=0 \quad (A.20)$$

$$\int_\theta \mathrm{A}_2\left[c_1\frac{\partial^2 w_0}{\partial x^2}+c_2\frac{\partial^2 w_0}{\partial\theta^2}\right]d\theta\Big|_{x=0,L}=0 \qquad or \qquad \delta\left(\frac{\partial w_0}{\partial x}\right)\Big|_{x=0,L}=0 \quad (A.21)$$

$$\int_\theta \mathrm{A}_2\left[c_1\frac{\partial^3 w_0}{\partial x^3}+c_2\frac{\partial^3 w_0}{\partial x\,\partial\theta^2}+c_5\frac{\partial^3 w_0}{\partial x\,\partial\theta^2}\right]d\theta\Big|_{x=0,L}=0 \qquad or \qquad \delta w_0\big|_{x=0,L}=0 \quad (A.22)$$

Boundary conditions for the edge with constant θ coefficient are as follows:

$$\int_x \mathrm{A}_2\left[a_3\frac{\partial u_0}{\partial\theta}+a_4\frac{\partial v_0}{\partial x}\right]dx\,\Big|_{\theta=0,\theta_0}=0 \qquad or \qquad \delta u_0\big|_{\theta=0,\theta_0}=0 \quad (A.23)$$

$$\int_x \mathrm{A}_2\left[b_1\frac{\partial u_0}{\partial x}+b_2\left(\frac{\partial v_0}{\partial\theta}+w_0\right)\right]dx\,\Big|_{\theta=0,\theta_0}=0 \qquad or \qquad \delta v_0\big|_{\theta=0,\theta_0}=0 \quad (A.24)$$

$$\int_x \mathrm{A}_2\left[c_3\frac{\partial^2 w_0}{\partial x^2}+c_4\frac{\partial^2 w_0}{\partial\theta^2}\right]dx\,\Big|_{\theta=0,\theta_0}=0 \qquad or \qquad \delta\left(\frac{\partial w_0}{\partial\theta}\right)\Big|_{\theta=0,\theta_0}=0 \quad (A.25)$$

$$\int_x \mathrm{A}_2\left[c_3\frac{\partial^3 w_0}{\partial x^2\partial\theta}+c_4\frac{\partial^3 w_0}{\partial\theta^3}+c_5\frac{\partial^3 w_0}{\partial x^2\partial\theta}\right]dx\,\Big|_{\theta=0,\theta_0}=0 \qquad or \qquad \delta w_0\big|_{\theta=0,\theta_0}=0 \quad (A.26)$$

The constants used in the above equations are as follows:

$$A_2=(1-l_s^2\nabla^2) \quad (A.27)$$

$$a_1=\frac{RhE_x}{1-\upsilon_{x\theta}\upsilon_{\theta x}} \quad , \quad a_2=\frac{hE_x\upsilon_{\theta x}}{1-\upsilon_{\theta x}\upsilon_{x\theta}} \quad , \quad a_3=\frac{hG_{x\theta}}{R} \quad , \quad a_4=hG_{x\theta} \quad (A.28)$$

$$b_1 = c_6 = \frac{hE_\theta \upsilon_{x\theta}}{1-\upsilon_{x\theta}\upsilon_{\theta x}} \quad , \quad b_2 = c_7 = \frac{hE_\theta}{R(1-\upsilon_{x\theta}\upsilon_{\theta x})} \quad , \quad b_3 = Ra_3 \quad , \quad b_4 = Ra_4 \tag{A.29}$$

$$c_1 = \frac{Rh_0^3 E_x}{12(1-\upsilon_{x\theta}\upsilon_{\theta x})} \quad , \quad c_2 = \frac{h_0^3 E_x \upsilon_{\theta x}}{12R(1-\upsilon_{\theta x}\upsilon_{x\theta})} \quad , \quad c_3 = \frac{h_0^3 E_\theta \upsilon_{x\theta}}{12R(1-\upsilon_{x\theta}\upsilon_{\theta x})} \tag{A.30}$$

$$c_4 = \frac{h_0^3 E_\theta}{12R^3(1-\upsilon_{x\theta}\upsilon_{\theta x})} \quad , \quad c_5 = \frac{h_0^3 G_{x\theta}}{3R} \tag{A.31}$$

Also, δT , δW are calculated as follows:

$$\delta T = \rho \int_x \int_\theta \left[\left(\frac{h^3 R}{12} \frac{\partial^4 w_0}{\partial x^2 \partial t^2} + \frac{h^3}{12R} \frac{\partial^4 w_0}{\partial \theta^2 \partial t^2} - hR \frac{\partial^2 w_0}{\partial t^2} \right) \delta w_0 - hR \left(\frac{\partial^2 u_0}{\partial t^2} \right) \delta u_0 - hR \left(\frac{\partial^2 v_0}{\partial t^2} \right) \delta v_0 \right] dx d\theta \tag{A.32}$$

$$\delta W = \int_\theta \int_x \left(f_x \delta u_0 + f_\theta \delta v_0 + f_z \delta w_0 \right) R dx d\theta \tag{A.33}$$

APPENDIX B

By substituting Eq. (31) into (17)-(19), the following equations are obtained:

$$A_2 \left[-a_1 U_{mn} \left(\frac{m\pi}{L} \right)^2 - a_3 U_{mn}(n)^2 - (a_2 + a_4) V_{mn} \left(\frac{m\pi}{L} \right)(n) + a_2 W_{mn} \left(\frac{m\pi}{L} \right) \right] \cos\left(\frac{m\pi}{L} x \right) \sin(n\theta) \mathrm{e}^{i\omega t} = -A_1 (\rho R h \omega^2 U_{mn}) \cos\left(\frac{m\pi}{L} x \right) \sin(n\theta) \mathrm{e}^{i\omega t} \tag{B.1}$$

$$A_2 \left[-(b_1 + b_3) U_{mn} \left(\frac{m\pi}{L} \right)(n) - b_4 V_{mn} \left(\frac{m\pi}{L} \right)^2 - \mathrm{b}_2 V_{mn}(n)^2 + b_2 W_{mn}(\mathrm{n}) \right] \sin\left(\frac{m\pi}{L} x \right) \cos(n\theta) \mathrm{e}^{i\omega t} = -A_1 \left(\rho h R \omega^2 V_{mn} \right) \sin\left(\frac{m\pi}{L} x \right) \cos(n\theta) \mathrm{e}^{i\omega t} \tag{B.2}$$

$$A_2 \left[c_1 W_{mn} \left(\frac{m\pi}{L} \right)^4 + (c_2 + c_3 + \mathrm{c}_5) W_{mn} \left(\frac{m\pi}{L} \right)^2 (n)^2 + c_4 W_{mn}(n)^4 - c_6 U_{mn} \left(\frac{m\pi}{L} \right) - c_7 \left(V_{mn}(\mathrm{n}) - W_{mn} \right) \right] \sin\left(\frac{m\pi}{L} x \right) \sin(n\theta) \mathrm{e}^{i\omega t} = A_1 \left[\frac{\rho h^3 R}{12} (\omega^2 W_{mn}) \left(\frac{m\pi}{L} \right)^2 + \frac{\rho h^3}{12R} (\omega^2 W_{mn})(\mathrm{n})^2 + \rho h R \omega^2 W_{mn} \right] \sin\left(\frac{m\pi}{L} x \right) \sin(n\theta) e^{i\omega t} \tag{B.3}$$

Components of the 3×3 matrix of coefficients $\left[F_{ij} \right] = \left[K - \omega^2 M \right]$ are defined as follows:

$$F_{11} = \left[1 + l_s^2 \left(\left(\frac{m\pi}{L} \right)^2 + \left(\frac{n}{R} \right)^2 \right) \right] \left[a_1 \left(\frac{m\pi}{L} \right)^2 + a_3 (n)^2 \right] - \left[1 + l_d^2 \left(\left(\frac{m\pi}{L} \right)^2 + \left(\frac{n}{R} \right)^2 \right) \right] \left(\rho R h \omega^2 \right) \tag{B.4}$$

$$F_{12}=\left[1+l_s^2\left(\left(\frac{m\pi}{L}\right)^2+\left(\frac{n}{R}\right)^2\right)\right]\left[\left(a_2+a_4\right)\left(\frac{m\pi}{L}\right)(n)\right] \tag{B.5}$$

$$F_{13}=\left[1+l_s^2\left(\left(\frac{m\pi}{L}\right)^2+\left(\frac{n}{R}\right)^2\right)\right]\left[a_2\left(\frac{m\pi}{L}\right)\right] \tag{B.6}$$

$$F_{21}=\left[1+l_s^2\left(\left(\frac{m\pi}{L}\right)^2+\left(\frac{n}{R}\right)^2\right)\right]\left[\left(b_1+b_3\right)\left(\frac{m\pi}{L}\right)(n)\right] \tag{B.7}$$

$$F_{22}=\left[1+l_s^2\left(\left(\frac{m\pi}{L}\right)^2+\left(\frac{n}{R}\right)^2\right)\right]\left[b_4\left(\frac{m\pi}{L}\right)^2+b_2(n)^2\right]-\left[1+l_d\left(\left(\frac{m\pi}{L}\right)^2+\left(\frac{n}{R}\right)^2\right)\right]\left(\rho Rh\omega^2\right) \tag{B.8}$$

$$F_{23}=\left[1+l_s^2\left(\left(\frac{m\pi}{L}\right)^2+\left(\frac{n}{R}\right)^2\right)\right]\left[b_2(n)\right] \tag{B.9}$$

$$F_{31}=\left[1+l_s^2\left(\left(\frac{m\pi}{L}\right)^2+\left(\frac{n}{R}\right)^2\right)\right]\left[c_6\left(\frac{m\pi}{L}\right)\right] \tag{B.10}$$

$$F_{32}=\left[1+l_s^2\left(\left(\frac{m\pi}{L}\right)^2+\left(\frac{n}{R}\right)^2\right)\right]\left[c_7(n)\right] \tag{B.11}$$

$$F_{33}=\left[1+l_s^2\left(\left(\frac{m\pi}{L}\right)^2+\left(\frac{n}{R}\right)^2\right)\right]\left[c_1\left(\frac{m\pi}{L}\right)^4+c_4(n)^4+\left(c_2+\mathrm{c}_3+\mathrm{c}_5\right)\left(\frac{m\pi}{L}\right)^2(n)^2+c_7\right]- \tag{B.12}$$
$$\left[1+l_d^2\left(\left(\frac{m\pi}{L}\right)^2+\left(\frac{n}{R}\right)^2\right)\right]\left[\frac{h^3R\omega^2}{12}\rho\left(\frac{m\pi}{L}\right)^2+\frac{h^3\omega^2}{12R}\rho(n)^2+\rho hR\omega^2\right]$$

REFERENCES

[1] Wada H., 2005, *Biomechanics at Micro- and Nanoscale Levels*, World Scientific Publishing Company.

[2] Alberts B., Bray D., Lewis J., Raff M., Roberts K., Watson J., 1994, *Molecular Biology of the Cell*, Garland Publishing, New York.

[3] Faber J., Portugal R., Ros L.P., 2006, Information processing in brain microtubules, *Biosystems* **83**: 1-9.

[4] Hawkins T., Mirigian M., Yasar M.S., Ross J.L., 2010, Mechanics of microtubules, *Journal of Biomechanics* **43**: 23-30.

[5] Pampaloni F., Florin E.L., 2008, Microtubule architecture: inspiration for novel carbon nanotube-based biomimetic materials, *Trends in Biotechnology* **26**(6): 302-310.

[6] Yuanwen G., Ming L.F., 2009, Small scale effects on the mechanical behaviors of protein microtubules based on the nonlocal elasticity theory, *Biochemical and Biophysical Research Communications* **387**: 467- 471.

[7] Tadi Beni Y., Abadyan M., 2013, Size-dependent pull-in instability of torsional nano-actuator, *Physica Scripta* **88**(5): 055801.

[8] Tadi Beni Y., Abadyan M., 2013, Use of strain gradient theory for modeling the size-dependent pull-in of rotational nano-mirror in the presence of molecular force, *International Journal of Modern Physics B* **27**: 1350083-1350101.

[9] TadiBeni Y., Koochi A., Abadyan M., 2011, Theoretical study of the effect of Casmir force, elastic boundary conditions and size dependency on the pull-in instability of beam-type NEMS, *Physica E* **43**: 979-988.

[10] Tadi Beni Y., Koochi A., Kazemi A.S., Abadyan M., 2012, Modeling the influence of surface effect and molecular force on pull-in voltage of rotational Nano–micro mirror using 2-DOF model, *Canadian Journal of Physics* **90**: 963-974.
[11] Sharma P., Zhang X., 2006, Impact of size-dependent non-local elastic strain on the electronic band structure of embedded quantum dots, *Journal Nanoengineering and Nanosystems* **220**: 17403499.
[12] Eringen A.C., 1983, On differential equations of nonlocal elasticity and solutions of screw dislocation and surface waves, *Journal of Applied Physics* **54**: 4703-4710.
[13] Gittes F., Mickey B., Nettleton J., Howard J., 1995, Flexural rigidity of microtubules and actin filaments measured from thermal fluctuation in shape, *Journal of Cell Biology* **120**: 923-934.
[14] Venier P., Maggs A.C., Carlier M.F., Pantaloni D., 1994, Analysis of microtubule rigidity using hydrodynamic flow and thermal fluctuations, *Journal of Biological Chemistry* **269**: 13353-13360.
[15] Vinckier A., Dumortier C., Engelborghs Y., Hellemans L., 1996, Dynamical and mechanical study of immobilized microtubule with atomic force microscopy, *Journal of Vacuum Science & Technology B* **14**: 1427-1431.
[16] Sirenko Y.M., Stroscio M.A., Kim K.W., 1996, Elastic vibration of microtubules in a fluid, *Physical Review E* **53**: 1003-1010.
[17] Wang C.Y., Ru C.Q., Mioduchowski A., 2006, Vibration of microtubules as orthotropic elastic shells, *Physica E* **35**: 48-56.
[18] Wang C.Y., Zhang L.C., 2008, Circumferential vibration of microtubules with long axial wavelength, *Journal of Biomechanics* **41**: 1892-1896.
[19] Shen H.S., 2011, Nonlinear vibration of microtubules in living cells, *Current Applied Physics* **11**: 812-821.
[20] Civalek Ö., Akgöz B., 2010, Free vibration analysis of microtubules as cytoskeleton components: nonlocal euler-bernoulli beam modeling, *Transaction B: Mechanical Engineering* **17**: 367-375.
[21] Heireche H., Tounsi A., Benhassaini H., Benzair A., Bendahmane M., Missouri M., Mokadem S., 2010, Nonlocal elasticity effect on vibration characteristics of protein microtubules, *Physica E* **42**: 2375-2379.
[22] Xiang P., Liew K.M., 2011, Free vibration analysis of microtubules based on an atomistic-continuum model, *Journal of Sound and Vibration* **331**: 213-230.
[23] Karimi Zeverdejani M., Tadi Beni Y., 2013, The nano scale vibration of protein microtubules based on modified strain gradient theory, *Current Applied Physics* **13**: 1566-1576.
[24] Lam D.C.C., Yang F., Chong A.C.M., Wang J., Tong P., 2003, Experiments and theory in strain gradient elasticity, *Journal of the Mechanics and Physics of Solids* **51**: 1477-1508.
[25] Fleck N., Muller G., Ashby M., Hutchinson J., 1994, Strain gradient plasticity: theory and experiment, *Acta Metallurgica et Materialia* **42**: 475-487.
[26] Stölken J., Evans A., 1998, A microbend test method for measuring the plasticity length scale, *Acta Materialia* **46**: 5109-5115.
[27] McElhaney K., Vlassak J., Nix W., 1998, Determination of indenter tip geometry and indentation contact area for depth-sensing indentation experiments, *Journal of Materials Research* **13**: 1300-1306.
[28] Nix W.D., Gao H., 1998, Indentation size effects in crystalline materials: a law for strain gradient plasticity, *Journal of the Mechanics and Physics of Solids* **46**: 411-425.
[29] Chong A., Lam D.C., 1999, Strain gradient plasticity effect in indentation hardness of polymers, *Journal of Materials Research* **14**: 4103-4110.
[30] Tadi Beni Y., Karimi Zeverdejani M., 2015, Free vibration of microtubules as elastic shell model based on modified couple stress theory, *Journal of Mechanics in Medicine and Biology* **15**(3):1550037-1550060.
[31] Askes H., Aifantis E.C., 2011, Gradient elasticity in statics and dynamics: An overview of formulations, length scale identification procedures, finite element implementations and new results, *International Journal of Solids and Structures* **48**: 1962-1990.
[32] Tuszynski J.A., Luchko T., Portet S., Dixon J.M., 2005, Anisotropic elastic properties of microtubules, *The European Physical Journal E* **17**: 29-35.
[33] De Pablo P.J., Schaap I..A.T., Mackintosh F.C., Schmidt C.F., 2003, Deformational collapse of microtubules on the nanometer scale, *Physical Review Letters* **91**: 098101.
[34] Sirenko Y. M., Stroscio M. A., Kim K. W., 1996, Elastic vibrations of microtubules in a fluid, *Physical Review E* **53**: 1003.
[35] Askes H., Aifantis E.C., 2009, Gradient elasticity and flexural wave dispersion in carbon Nanotubes, *Physical Review B* **80**: 195412.
[36] Bennett T., Gitman I., Askes H., 2007, Elasticity theories with higher-order gradients of inertia and stiffness for the modeling of wave dispersion in laminates, *International Journal of Fracture* **148**: 185-193.
[37] Gitman I., Askes H., Aifantis E.C., 2005, The representative volume size in static and dynamic micro-macro transitions, *International Journal of Fracture* **135**: 3-9.
[38] Wang Q., 2005, Wave propagation in carbon nanotubes via nonlocal continuum mechanics, *Journal of Applied Physics* **98**: 124301.

[39] Civalek O., Demir C., Akgoz B., 2010, Free vibration and bending analyses of cantilever microtubules based on nonlocal continuum model, *Mathematical and Computational Applications* **15**: 289-298.

[40] Heireche H., Tounsi A., Benhassaini H., Benzair A., Bendahmane M., Missouri M., Mokadem S., 2010, Nonlocal elasticity effect on vibration characteristics of protein microtubules, *Physica E* **42**: 2375-2379.

[41] Shen H. S., 2010, Nonlocal shear deformable shell model for postbuckling of axially compressed microtubules embedded in an elastic medium, *Biomechanics and Modeling in Mechanobiology* **9**: 345-357.

[42] Shen H. S., 2010, Buckling and postbuckling of radially loaded microtubules by nonlocal shear deformable shell model, *Journal of Theoretical Biology* **264**: 386-394.

[43] Park S., Gao X., 2006, Bernoulli–Euler beam model based on a modified couple stress theory, *Journal of Micromechanics and Microengineering* **16**: 2355-2359.

[44] Maranganti R., Sharma P., 2007, A novel atomistic approach to determine strain-gradient elasticity constants: Tabulation and comparison for various metals, semiconductors, silica, polymers and the (ir) relevance for nanotechnologies, *Journal of the Mechanics and Physics of Solids* **55**: 1823-1852.

[45] Duan W., Wang C.M., Zhang Y., 2007, Calibration of nonlocal scaling effect parameter for free vibration of carbon nanotubes by molecular dynamics, *Journal of Applied Physics* **101**: 024305-024307.

[46] Chan K., Zhao Y., 2011, The dispersion characteristics of the waves propagating in a spinning single-walled carbon nanotube, *Science China Physics, Mechanics & Astronomy* **54**: 1854-1865.

[47] Shi Y.J., Guo W.L., Ru C.Q., 2008, Relevance of timoshenko-beam model to microtubules of low shear modulus, *Physica E* **41**: 213-219.